Cross-Layer Designs and Analysis of Adaptive-rate Transmission and ARQ for Free-Space Optical Communications

Vuong V. Mai, ***Student Member, IEEE,*** **and Anh T. Pham,** ***Senior Member, IEEE***

Computer Communications Lab., The University of Aizu, Aizuwakamatsu, Fukushima, Japan 965-8580

DOI: 10.1109/JPHOT.2009.XXXXXXX

Manuscript received March 3, 2008; revised November 10, 2008. First published December 10, 2008. Current version published February 25, 2009. Corresponding author: Vuong V. Mai (e-mail: m.v.vuong@ieee.org).

Abstract: The impact of atmospheric turbulence is one of the most challenging issues for the widespread deployment of Free-space optical (FSO) communication systems. To enhance the systems' performance, adaptive-rate (AR) transmission and automatic repeat request (ARQ) have been separately considered at the physical and data link control layers. This paper introduces a framework of cross-layer design, analysis and optimization for FSO communication systems, in which ARQ and adaptive-rate transmission are jointly integrated to further improve the overall system performance over atmospheric turbulence channels. Two cross-layer designs are considered: (i) AR and standard-ARQ, and (ii) AR and ARQ with frame combining. In addition, we newly develop a Markov chain model-based cross-layer analysis for evaluating the system performance. System performance metrics, including spectral efficiency, maximum expected number of transmissions and outage probability, are analytically studied under the presence of atmospheric turbulence. In numerical results, how the cross-layer designs significantly outperform conventional ones is quantitatively shown. Furthermore, we discuss a cross-layer optimization of selecting the ARQ persistence level for the trade-off between the spectral efficiency and number of transmissions.

Index Terms: Free-space Optical (FSO) Communications, Atmospheric Turbulence Channel, Automatic Repeat Request (ARQ), Adaptive-rate Transmission, Cross-layer Design.

1. Introduction

Free-space optical (FSO) communications is a wireless communication technology based on the propagation of light in free space. Achieving data rates comparable to that of fiber optics without incurring exorbitant costs and requiring significant amount of time for installation, FSO is able to provide a low-cost, time-constrained and high-bandwidth connectivity in various network scenarios. In metropolitan area networks (MANs), FSO can be deployed to extend an existing metro ring or to connect new networks, e.g., 5G networks; in enterprise, it can be used to interconnect local area networks (LANs); and it can also be used as a scalable and cost effective solution for last-mile connectivity [1], [2].

The performance of FSO systems is, nevertheless, severely degraded by the impact of atmospheric turbulence, which results in the fluctuations of signal intensity and phase [3]–[6]. This is one of the most challenging issues for the widespread deployment the FSO in communication networks. Many techniques have been proposed over the last decade to improve the performance of FSO systems (for more details, see [2]). Among them, link adaptation technologies, such

as adaptive-rate (AR) transmission and automatic repeat request (ARQ), have recently received significant attention due to their advantages of efficiency, effectiveness with no additional physical infrastructures required [7]–[14]. In previous studies, however, AR and ARQ are separately considered for FSO systems. The goal of this paper is to introduce a framework of cross-layer design, analysis and optimization for FSO systems, in which ARQ in data link control (DLC) layer and AR transmission in physical (PHY) layer are integrated to offer an effective solution to improve the overall system performance over atmospheric turbulence channels.

1.1. Related Works & Motivations

Recently, application of AR and ARQ in FSO communications has been separately studied. It is seen that AR transmission is the key factor for increasing the FSO system spectral efficiency [7]–[10]. Other studies also revealed that by allowing retransmission of erroneous frames, ARQ offers an efficient control mechanism for reliable transmissions in FSO systems [11]–[14].

In the domain of radio-frequency (RF) communications, the use of integrated AR and ARQ has become a standard in wireless networks thanks to the fact that the system spectral efficiency would be significantly improved by jointly exploiting the adaptability of AR to the wireless noisy channel conditions and the error control capability of ARQ [15]–[18]. There are, however, two significant differences when applying these techniques in FSO and RF communications.

First, under the impact of various channel impairments, including fading channels and interferences [19], the more aggressive error control method, Hybrid-ARQ (H-ARQ), which achieves better reliability by combining ARQ and forward error correction (FEC) codes, is preferable to standard ARQ for AR/ARQ cross-layer design [18]. However, H-ARQ results in more system complexity, additional signaling and especially, large overhead. In FSO communications however, the impact of channel impairments is less severe in comparison with that of RF, using H-ARQ with large overhead would be not efficient.

Secondly, due to the fast fading channel and low speed transmission in RF communications, the period that AR stays in a transmission rate may not be long enough to cover whole ARQ process of a frame, including the initial transmission and retransmissions. Therefore, previous AR/ARQ cross-layer analysis frameworks for RF communication assumed that the transmissions of a frame may happen at different transmission rates [15], [17]. In FSO communication, nevertheless, the atmospheric turbulence changes more slowly, and with the higher data rate, it is more plausible to assume that these transmissions can be covered by the period staying in a transmission rate[1].

1.2. Our Contributions

Motivated by the above discussion, the main goal of this paper is to provide a unified view of AR/ARQ cross-layer design, analysis and optimization for FSO communication systems. To the best of our knowledge, this is the first study, which is the extension of our previously published papers [20], [21], to consider the unique characteristics of FSO systems in design and analysis of AR, ARQ and joint AR/ARQ as well. More specifically, the contributions of this paper can be summarized as follows:

1) We promote to use the standard-ARQ, which is sufficiently reliable, yet simple and less overhead, for FSO systems. Furthermore, we introduce another method to improve the reliability of standard-ARQ without using FEC. This is realized by implementing frame combining at the receiver. To this end, two cross-layer designs are proposed: (i) AR and standard-ARQ (AR/ARQ), and (ii) AR and ARQ with frame combining (AR/ARQ-FC).
2) To reflect the critical assumption of correlation between operations of AR and ARQ in FSO systems, we newly develop a novel Markov chain model-based cross-layer analysis. We also consider in the model the time-varying behavior of atmospheric turbulence channel, which

[1]Consider, for example, a 1 Gb/s FSO communication system whose frame size in DLC layer is 1080 bits. It takes nearly 1 μs to transmit one frame. As the atmospheric turbulence changes slowly, correlation time is typically 1 to 10 ms or longer [7], a transmission rate period may cover at less 1000 frame transmissions.

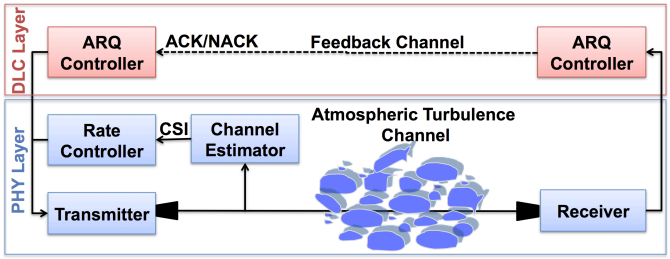

Fig. 1. Modeling of a FSO communication system combining AR at the PHY layer with ARQ at the DLC layer.

was often omitted in previous FSO's studies for modeling AR transmission [7]–[10]. As in the cross-layer design, we observe frame-by-frame transmissions that capture the memory properties of channel, it is important to include the time-varying behavior of atmospheric turbulence channel in the analysis for more accuracy.

3) The proposed model allows the derivation of the system performance metrics, including spectral efficiency, maximum expected number of transmissions and outage probability. Based on these metrics, we discuss a cross-layer optimization, where the ARQ persistent level is selected by a trade-off between the number of transmissions and the spectral efficiency. Numerical results confirm the superiority of cross-layer designs over conventional ones, and that AR/ARQ-FC with the optimal persistence level is more efficient than AR/ARQ.

The remainder of the paper is organized as follows. The system description is presented in Sect. 2. In Sect. 3, the conventional and cross-layer designs are introduced. The Markov chain models and performance metrics are derived in Sect. 4. Numerical results are given in Sect. 5. Finally, Sect. 6 concludes the paper.

$Notation$: $\Gamma(.)$ and $\Gamma_l(\cdot,\cdot)$ are the ordinary and lower incomplete Gamma functions, respectively; $K_v(\cdot)$ is the modified Bessel function of second kind and order v-th; $G_{p,q}^{m,n}[\cdot]$ is the Meijer's G-function; $B(\cdot,\cdot)$ is the Beta function.

2. System Descriptions

Figure 1 shows a FSO communication system that consists of a transmitter, a receiver, and a propagation path through the atmospheric turbulence channel. In addition, the system employs the link adaptation technologies, including AR at the PHY layer and ARQ at the DLC layer.

2.1. Channel Model

The atmospheric turbulence causes irradiance fluctuations, i.e., scintillation, on the received signals propagating along a horizontal path between the transmitter and receiver. The main cause of scintillation is small temperature variations in the atmosphere, which results in refraction-index random variations [3]–[6]. Over the years, many statistical models have been proposed to describe the atmospheric turbulence channels for varying degrees of strength. The most widely accepted distributions are the Log-Normal (LN) and Gamma-Gamma (GG) models. Experimental studies support the fact that the LN model is valid in weak turbulence regime, while the GG model is accepted to be valid in all turbulence regimes. The GG distribution is used to model the two independent contributions of the small-scale and large-scale of turbulence, assuming a Gamma process governs each of them. The GG distribution is given by [5]

$$f_H(h) = \frac{2(\alpha\beta)^{\frac{\alpha+\beta}{2}}}{\Gamma(\alpha)\Gamma(\beta)} h^{\frac{\alpha+\beta}{2}-1} K_{\alpha-\beta}\left(2\sqrt{\alpha\beta h}\right), \quad (1)$$

where h is the signal intensity, α and β are parameters directly related to the effects induced by the large-scale and small-scale scattering, respectively. These parameters are given by [6]

$$\alpha = \left\{ \exp\left[\frac{0.49\sigma_R^2}{\left(1+1.11\sigma_R^{12/5}\right)^{7/6}} \right] - 1 \right\}^{-1},$$
$$\beta = \left\{ \exp\left[\frac{0.51\sigma_R^2}{\left(1+0.69\sigma_R^{12/5}\right)^{5/6}} \right] - 1 \right\}^{-1}, \quad (2)$$

where σ_R^2 is the Rytov variance, which is in fact the scintillation index of an unbounded plane wave in the weak turbulence regime, given by $\sigma_R^2 = 1.23\left(\frac{2\pi}{\lambda}\right)^{7/6} C_n^2 d^{11/6}$ [3], in which λ is the optical wavelength, d is the transmission distance, and C_n^2 is the altitude-dependent index of the refractive structure parameter. In general, C_n^2 varies from 10^{-13} m$^{-2/3}$ to 10^{-17} m$^{-2/3}$. Typically, weak turbulence fluctuations are associated with $\sigma_R^2 < 1$, moderate with $\sigma_R^2 \approx 1$, strong with $\sigma_R^2 > 1$, and the saturation regime is defined by $\sigma_R^2 \to \infty$ [7], [22].

The instantaneous received electrical signal-to-noise ratio (SNR) can be expressed as $\gamma = \overline{\gamma} h^2$, where $\overline{\gamma}$ is the average electrical SNR per symbol. Using (1), after transformation of random variable h, we obtain the PDF of γ as

$$f_\gamma(\gamma) = \frac{(\alpha\beta)^{\frac{\alpha+\beta}{2}}}{\Gamma(\alpha)\Gamma(\beta)\overline{\gamma}^{\frac{\alpha+\beta}{4}}} \gamma^{\frac{\alpha+\beta}{4}-1} K_{\alpha-\beta}\left(2\sqrt{\alpha\beta\sqrt{\frac{\gamma}{\overline{\gamma}}}}\right), \quad (3)$$

while its cumulative distribution function (CDF) can be expressed as [9]

$$F_\gamma(\gamma) = \frac{1}{\Gamma(\alpha)\Gamma(\beta)} G_{1,3}^{2,1}\left[\alpha\beta\sqrt{\frac{\gamma}{\overline{\gamma}}}\Big|_{\alpha,\beta,0}^{1}\right]. \quad (4)$$

2.2. Adaptive-rate Transmission

In Fig. 1, due to channel reciprocity in bidirectional fading channels[2], it can be assumed that the transmitter has perfect and immediate knowledge of the channel state information (CSI) at the receiver. Based on CSI, the transmission rate can be adjusted dynamically at the transmitter.

We also assume that there are $(\mathfrak{m}+1)$ available transmission rates: $\{\Re_0, \Re_1, ..., \Re_\mathfrak{m}\}$; the range of SNR is divided into $(\mathfrak{m}+1)$ set of non-overlapping intervals: $\{[\gamma_0, \gamma_1), [\gamma_1, \gamma_2), ..., [\gamma_\mathfrak{m}, \gamma_{\mathfrak{m}+1})\}$, where $\Re_0 = 0$, $\gamma_0 = 0$ and $\gamma_{\mathfrak{m}+1} = \infty$. Each interval is associated with a transmission rate according to the following rule:

$$R = \Re_i, \ \ \gamma \in [\gamma_i, \gamma_{i+1}). \quad (5)$$

In adaptive-rate transmission, depending on the FSO channel conditions, we change the signal constellation size for the fixed symbol rate. Practically, this flexibility could be addressed via a software-based configuration or implementation of the operating function at the transmitter [24]. When the channel conditions are favorable we increase the constellation size, we decrease it when channel conditions are not favorable, and we do not transmit at all when the intensity channel coefficients are below the irradiance threshold, i.e., $R = \Re_0 = 0, \ \ \gamma \in [\gamma_0, \gamma_1)$.

In FSO communication systems, to realize AR transmission, most of previous studies suggested to use multilevel modulations, e.g., M-PAM [7], M-PSK [9], or M-QAM [10]. In the rest of this paper, we apply the adaptive-rate transmission described above to a commonly used modulation scheme, M-QAM. As the assumption of $(\mathfrak{m}+1)$ available transmission rates, M-QAM with $M =$

[2]The channel reciprocity connotes that the received signal levels at both link ends are similar or, ideally, identical. A measurement of reciprocity was reported in [23] for atmospheric optical links.

$2^i, i = 1, 2, ..., \mathfrak{m}$, is assumed. Hence, for a fixed symbol rate of R_0, the transmission rate is given as: $\Re_i = R_0 \log_2(M)$.

2.3. Automatic Repeat Request

ARQ is a frame-oriented feedback-based data transmission technique at the DLC layer. Data frames are appended with an error-detection code and sent to the receiver. After receiving a frame, the receiver checks for errors in the received data. If the frame is received without any errors, the receiver sends an acknowledgement (ACK) on a feedback channel[3] to the transmitter. If there are errors, the receiver sends a negative acknowledgement (NACK) asking for a retransmission, and this process is continued until the frame is successfully received or the maximum number of retransmissions, i.e., persistence level, is reached. In the latter case, the frame is declared to be lost, and it may be kept in the buffer for a later transmission or simply discarded.

Besides the standard-ARQ protocol, the Hybrid-ARQ protocols have been also considered. In these protocols, both error-detection and error-correction codes are used. If the number of errors in a received frame is within the error correcting capability of the code, the errors will be corrected. If the receiver is unable to correct the errors, it asks for a retransmission. Obviously, H-ARQ would provide higher reliability than the conventional ARQ. However, H-ARQ requires more complexity, signaling and overhead.

As explained in Section I, we consider the standard-ARQ, which is sufficiently reliable, yet simple and less overhead, for FSO systems. Furthermore, we introduce another method to improve the reliability of standard-ARQ without using FEC. This is realized by implementing frame combining at the receiver. In particular, when operating ARQ in a frame, the receiver stores all copies of previous transmissions, including the initial transmission and retransmissions; if the next retransmission happens, the received frame will be combined with the stored copies. To this end, the likelihood of successfully retransmitting frames would be improved. In practical systems, as the receiver always has a buffer to store frames before delivering them to end-users, storing and combining frames for operating such method do not introduce a significant system cost increase. Moreover, the method can also avoid the requirement of additional signaling and overhead.

3. Switching Thresholds Designs

In AR transmission, $\{\gamma_i \mid i = 0, 1, ..., \mathfrak{m}+1\}$ are switching thresholds. Being used in the searching algorithm (i.e., (5)) for the selection of transmission rate, switching thresholds play an important role in the system operation. This Section discusses how to design the thresholds. Besides the conventional approach, cross-layer approaches are introduced for enhancing the system performance.

3.1. Conventional Design

The aim of AR is to provide the highest possible transmission rate while maintaining a required QoS. Conventionally, in most previous studies of FSO communications [7]–[10], the performance of PHY layer-based QoS is considered. In particular, a target bit-error rate (BER_0) is considered as the level of required QoS, and the design problem can be formally formulated as

$$\begin{aligned} &\max \ M \mid M = 2^i, i = 1, 2, ..., \mathfrak{m} \\ &\text{subject to } \text{BER}(M, \gamma) \leq \text{BER}_0, \end{aligned} \tag{6}$$

where $\text{BER}(M, \gamma)$ is the conditional BER. This is calculated based on the conditional BER of M-QAM over the Additive white Gaussian noise (AWGN) channel, which is well approximated as

[3]We assume that there is an erroneous feedback channel available between the receiver and transmitter. In practical, the feedback channel can be realized by using one link of bi-directional FSO link.

follows [25]

$$\text{BER}(M,\gamma) \cong 0.2\text{exp}\left(-\frac{3\gamma}{2(M-1)}\right). \quad (7)$$

From (6) and (7), the switching thresholds are derived as

$$\gamma_i = \frac{-2(2^i-1)}{3}\ln\left(5\text{BER}_0\right). \quad (8)$$

3.2. Cross-layer Designs

Besides the conventional design, we introduce cross-layer approaches for designing the thresholds. In here, the QoS provided by DLC layer is considered. Specifically, this design takes into account the error control capability of ARQ, and uses a target layer frame-error rate (FER_0) as the required QoS. First, we consider the conditional frame error rate, $\text{FER}(M,\gamma)$, where frames are formed with L transmitted bits. Without any coding on this frame, the frame error probability at a given instantaneous SNR is given as

$$\text{FER}(M,\gamma) = 1-[1-\text{BER}(M,\gamma)]^L. \quad (9)$$

By applying a probability union-bound, we have: $1-[1-\text{BER}(M,\gamma)]^L \leq L\text{BER}(M,\gamma)$. The bound gets tighter as $\text{BER}(M,\gamma)$ decreases when $\gamma \to \infty$. So, we can derive a closed-form approximation for the conditional FER as

$$\text{FER}(M,\gamma) \cong L\text{BER}(M,\gamma) \cong 0.2L\text{exp}\left(-\frac{3\gamma}{2(M-1)}\right). \quad (10)$$

By using the probability union-bound, we can find the connection between the target FER and the target BER as

$$\text{FER}_0 = 1-(1-\text{BER}_0)^L \approx L\text{BER}_0. \quad (11)$$

Next, we determine how to design the switching thresholds, considering that ARQ is implemented in the DLC layer. We set the maximum number of ARQ re-transmissions to K. It means that a frame is considered to be lost only if it does not get through the links after $(K+1)$ transmissions. To this end, the conditional frame error rate can be translated into a new equivalent one, as follows

$$\text{FER}^\star(M,\gamma) = \prod_{k=1}^{K+1} P(k), \quad (12)$$

where $P(k)$ is the conditional frame error rate of the k-th transmission. Consequently, the switching thresholds can be designed based on the following conditions

$$\begin{aligned} &\max\ M \mid M = 2^i, i = 1,2,...,\mathfrak{m} \\ &\text{subject to } \text{FER}^\star(M,\gamma) \leq \text{FER}_0, \end{aligned} \quad (13)$$

We describe below the cross-layer design for two different ARQ protocols: (i) the conventional ARQ[4], and (ii) ARQ with frame combining.

3.2.1. Standard-ARQ

In standard-ARQ protocol, the receiver considers only the most recently received frame. So, the conditional frame error rate of the k-th transmission does not depend on previous transmissions.

$$P(1) = P(2) = ... = P(K+1) = \text{FER}(M,\gamma). \quad (14)$$

[4]We have introduced this design in [20] and [21] for FSO and hybrid FSO/RF communications systems, respectively.

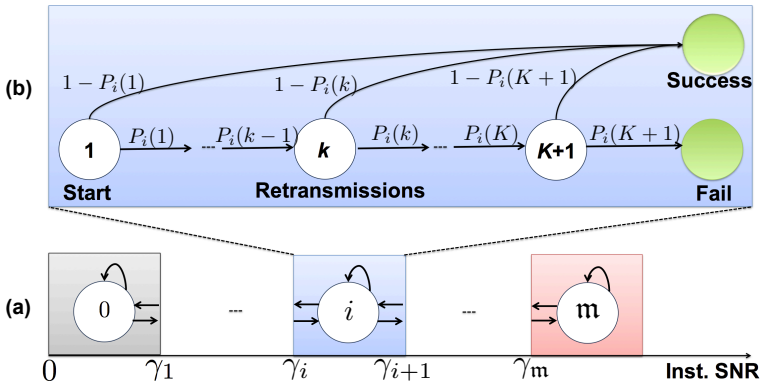

Fig. 2. Markov chain for modeling the operations of (a) AR transmission and (b) ARQ protocol.

By submitting (14) and (10) into (12), we have

$$\text{FER}^{\star}(M,\gamma) = \text{FER}(M,\gamma)^{K+1} = \left(0.2L\exp\left(-\frac{3\gamma}{2(M-1)}\right)\right)^{K+1}. \tag{15}$$

From (13) and (15), the switching thresholds are derived as

$$\gamma_i = \frac{-2(2^i-1)}{3}\ln\left(\frac{5\text{FER}_0^{\frac{1}{K+1}}}{L}\right). \tag{16}$$

3.2.2. ARQ with Frame Combining

The receiver is assumed to perform a maximum ratio combiner on all the received frames; thus, the SNR of k-th transmission is accumulated over k rounds. Therefore, the conditional frame error rate of the k-th transmission can be approximated as [26]

$$P(k) \approx \text{FER}(M,k\gamma),\ k=1,2,...,K+1. \tag{17}$$

By substituting (17) and (10) into (12), we have

$$\text{FER}^{\star}(M,\gamma) = \prod_{k=1}^{K+1} L0.2\exp\left(-\frac{3k\gamma}{2(M-1)}\right) = (0.2L)^{K+1}\exp\left(-\frac{3(K+1)(K+2)\gamma}{4(M-1)}\right). \tag{18}$$

From (13) and (18), the switching thresholds are derived as

$$\gamma_i = \frac{-4(2^i-1)}{3(K+1)(K+2)}\ln\left(\frac{\text{FER}_0}{(0.2L)^{K+1}}\right). \tag{19}$$

4. Cross-layer Analysis

In this study, we newly develop a Markov chain model-based framework to analytically study the system performance. Our framework differs from related cross-layer analysis (for RF wireless communications [15], [17]) in that it reflects the assumption that all possible transmissions of a frame can be completed within the period in which a single transmission rate is set. In addition, for the higher accurate performance evaluation, additional time-varying behavior of atmospheric turbulence, which is omitted in previous FSO studies for modeling AR transmission [7]–[10], is added in the proposed model.

4.1. AR Transmission Modeling

The operation of AR can be modeled as a Markov chain shown in Fig. 2(a). There are $(\mathrm{m}+1)$ states; each state expresses a transmission rate, which increases gradually from left to right. In a slow fading channel, we can assume that the transitions only happen between adjacent states. Whenever the channel quality degrades, the system moves to a lower-rate state. In cases when the channel quality does not change (or gets better), the system stays at the current state (or goes back the previous higher-rate state). In the worst channel quality, the system selects the zero-rate state, i.e., leftmost state. As a result, we can construct a state transition matrix, $(\mathrm{m}+1)\times(\mathrm{m}+1)$ **Q**, as follows

$$\begin{bmatrix} \mathbf{q}_{0,0} & \mathbf{q}_{0,1} & 0 & \cdots & 0 & 0 & 0 \\ \mathbf{q}_{1,0} & \mathbf{q}_{1,1} & \mathbf{q}_{1,2} & \cdots & 0 & 0 & 0 \\ \vdots & \vdots & \vdots & \ddots & \vdots & \vdots & \vdots \\ 0 & 0 & 0 & \cdots & \mathbf{q}_{\mathrm{m}-1,\mathrm{m}-2} & \mathbf{q}_{\mathrm{m}-1,\mathrm{m}-1} & \mathbf{q}_{\mathrm{m}-1,\mathrm{m}} \\ 0 & 0 & 0 & \cdots & 0 & \mathbf{q}_{\mathrm{m},\mathrm{m}-1} & \mathbf{q}_{\mathrm{m},\mathrm{m}} \end{bmatrix}, \tag{20}$$

where $q_{i,j}$ is the state transition probability from a transmission rate of i to one of j. In order to find the state transition probabilities, we use experimental results supporting the time-varying behavior of atmospheric turbulence. In particular, at any SNR threshold level of γ_{th}, there is the function of level crossing rate (LCR), which is defined as the average number of times per second that the received SNR of system passes either upward or downward the level of γ_{th}. The LCR is inversely proportional to the coherence time, t_0, yet increases as the turbulence becomes stronger, and can be obtained as follows [27]

$$N(\gamma_{th}) = \frac{1}{4\pi t_0}\exp\left(\frac{1}{2\left(1-\mathrm{e}^{4\sigma_S^2}\right)}\left(\frac{\gamma_{th}-\overline{\gamma}}{\overline{\gamma}}\right)^2\right), \tag{21}$$

where σ_S^2 is log intensity variance, which describes the strength of turbulence. The relation between σ_S^2 and σ_R^2 is given by Eq. (10) of [28].

Now, the probability of moving from a transmission rate of i to one of j can be calculated as

$$\mathbf{q}_{i,j} = \begin{cases} 0, & |i-j| \geq 2 \\ \frac{N(\gamma_{i+1})T_i}{P_i}, & j = i+1 \\ \frac{N(\gamma_i)T_i}{P_i}, & j = i-1 \\ 1-\mathbf{q}_{i,i+1}-\mathbf{q}_{i,i-1}, & j = i \text{ and } j \notin \{0,\mathrm{m}\} \\ 1-\mathbf{q}_{\mathrm{m},\mathrm{m}-1}, & j = i = \mathrm{m} \\ 1-\mathbf{q}_{0,1}, & j = i = 0 \end{cases}, \tag{22}$$

where $T_i = L/(iR_0)$ is the frame transmission time at the rate of i with R_0 is the symbol rate; P_i is the probability that the transmission rate of i is selected [29],

$$P_i = \int_{\gamma_i}^{\gamma_{i+1}} f_\gamma(\gamma)d\gamma = F_\gamma(\gamma_{i+1}) - F_\gamma(\gamma_i), \tag{23}$$

where $f_\gamma(.)$ and $F_\gamma(.)$ are PDF and CDF of γ given by (3) and (4).

Let **P**= [p_1 p_2 ... $p_{\mathrm{m}+1}$] be the matrix of steady-state probabilities, where p_i is the probability of the i-th state in the equilibrium. Generally, following Markov chain theory, we have

$$\begin{cases} \mathbf{P} = \mathbf{PQ}, \\ \sum_{i=1}^{\mathrm{m}+1} p_i = 1, \end{cases} \tag{24}$$

In order to calculate the elements of **P**, we transform (24) into a basic set of linear equations and then solve the equations by using the standard Gaussian elimination.

4.2. ARQ Modelling

As it is assumed that the period that AR stays in a transmission rate can cover all possible transmissions of a frame, for each AR state of i in Fig. 2(a), we develop a reducible discrete-time Markov chain for modeling the operation of ARQ. In the model shown in Fig. 2(b), each state is defined with the index denoting the transmission order, i.e., k. The inter-transition probabilities between these states are in fact the frame error probabilities, i.e., $P_i(k)$. Moreover, **Success** and **Fail** states are defined to represent successful and failed transmission, respectively. The resulting model is a special case of a Markov chain, which has two absorbing states, including **Success** and **Fail**, and transient states (i.e., other states)[5]. For the further analysis, we consider $(K+1)\times(K+1)$ **T** matrix: this is state transition matrix from transient states to transient states,

$$\mathbf{T} = \begin{bmatrix} 0 & P_i(1) & 0 & 0 & \cdots & 0 & 0 \\ 0 & 0 & P_i(2) & 0 & \cdots & 0 & 0 \\ \vdots & \vdots & \vdots & \vdots & \ddots & \vdots & \vdots \\ 0 & 0 & 0 & 0 & \cdots & 0 & P_i(K) \\ 0 & 0 & 0 & 0 & \cdots & 0 & 0 \end{bmatrix}. \tag{25}$$

The fundamental matrix **E** in the reducible discrete-time Markov chain model is given as

$$\mathbf{E} = (\mathbf{I} - \mathbf{T})^{-1}, \tag{26}$$

where **I** is an $(K+1)\times(K+1)$ identity matrix.

Generally, each element of the fundamental matrix denotes the average number of visits to transient states before transiting to any absorbing state. In particular, the sum of the a-th row elements of **E** (i.e., $\sum_{b=1}^{K+1}\mathbf{E}_{a,b}$) denotes the average number of total transmissions until being absorbed into either **Success** and **Fail** states when starting at a transient state a. Without loss of generality, we can assume that state "1" is always the starting state of the chain. Hence, we can calculate the expected number of transmissions for each frame, until it is successfully transmitted or discarded, as follows

$$N_i = \sum_{b=1}^{K+1}\mathbf{E}_{1,b}. \tag{27}$$

From above analysis, it is possible to calculate N_i if all $P_i(k)$ are known. The closed-form expressions of $P_i(k)$ are derived in the Appendix for two cases: (i) standard-ARQ, and (ii) ARQ with frame combining.

4.3. Performance Metrics

4.3.1. Spectral Efficiency

When the system operates in the AR state of i, each transmitted symbol will carry $\Re_i$ information bits. We assume a Nyquist pulse shaping filter with bandwidth $B = 1/R_0$. Hence, in the favorable scenario that all frames are assumed to be successfully transmitted in their initial transmissions, the achievable spectral efficiency (bit rate per unit bandwidth) is given by [7]

$$\mathbb{S}_{\text{achievable}} = \frac{1}{R_0}\sum_{i=1}^{\mathrm{m}+1} p_i\Re_i. \tag{28}$$

In the state i each frame (and thus each information bit) may be transmitted N_i times due to the operation of ARQ. Consequently, the average spectral efficiency of cross-layer design can be expressed as

$$\mathbb{S}_{\text{average}} = \frac{1}{R_0}\sum_{i=1}^{\mathrm{m}+1}\frac{1}{N_i}p_i\Re_i. \tag{29}$$

[5]The theory of reducible discrete-time Markov chain and its results used in this paper can be found in [30].

4.3.2. Maximum Expected Number of Transmissions

We define the metric expressing the cost of using ARQ,

$$\mathbb{N}_{\text{max}} = \max(N_1, N_2, ..., N_{\mathfrak{m}+1}). \tag{30}$$

This is the maximum expected number of transmissions that possibly happens in a AR state. It will be used when analyzing a trade-off between the number of transmissions and achievable spectral efficiency.

4.3.3. Outage Probability

In AR systems, the outage probability is defined as the probability that no data is transmitted due to the bad channel quality [10]. So, this can be calculated as the probability of zero-rate state in Fig. 2(a),

$$\mathbb{P}_{\text{outage}} = p_1. \tag{31}$$

5. Numerical Results and Discussions

In this section, we evaluate the performance of the proposed cross-layer designs. We also compare the designs with conventional designs, including fixed-rate, and adaptive-rate only (AR). The derived analytical framework is applied for each design as follows: (i) for adaptive rate systems: the switching thresholds obtained from (19), (16), and (8) are used in (20)–(31) for AR/ARQ-FC, AR/ARQ, and AR, respectively, (ii) for fixed-rate systems: consider a fixed M-QAM, there is only one threshold obtained from (8): γ_i, $i = \log_2(M)$, and a simplified Markov chain with two states[6] can be used to model the operation of the system.

The system parameters are given in Table I. Note that low persistence level, $K \leq 3$, is assume to avoid high delay and energy consumption in frame transmissions; for atmospheric turbulence channels, the Rytov variances $\sigma_R^2 = 0.59$, $\sigma_R^2 = 0.9$, and $\sigma_R^2 = 1.2$ are assumed for the weak, moderate and strong turbulence conditions, respectively. In Fig. 3, we consider the achievable

TABLE I
SYSTEM PARAMETERS

Name	Symbol	Value
Signal constellation size	M	2,4,8,16,32
Persistence level	K	1,2,3
Atmospheric coherence time	t_0	1 ms
Frame size	L	1080 bits
Symbol rate	R_0	200 Msps
Target bit-error rate	BER_0	10^{-5}
Target frame-error rate	FER_0	10^{-2}
Rytov variances	σ_R^2	0.59, 0.9, 1.2

spectral efficiency as a function of average electrical SNR per symbol, i.e., $\overline{\gamma}$, and compare the performance of adaptive-rate and fixed-rate systems. In fixed-rate cases, there are remarkable points: (i) a system with a high signal constellation size may achieve a high maximum spectral efficiency, yet it requires high SNR to reach this value, and (ii) with a low signal constellation size, the system may only achieve a low maximum spectral efficiency, yet it requires low SNR to reach this value. So, it is hard to determine a fixed-rate system that can offer the high maximum spectral efficiency in the low required SNR.

On the other hand, compared to the fixed-rate cases, adaptive-rate systems have significantly better performance thanks to the adaptive-rate strategy. For example, to achieve the spectral

[6]State 1: $\gamma \in [0, \gamma_i)$ and $R = 0$; state 2: $\gamma \in [\gamma_i, \infty)$ and $R = \Re_i$.

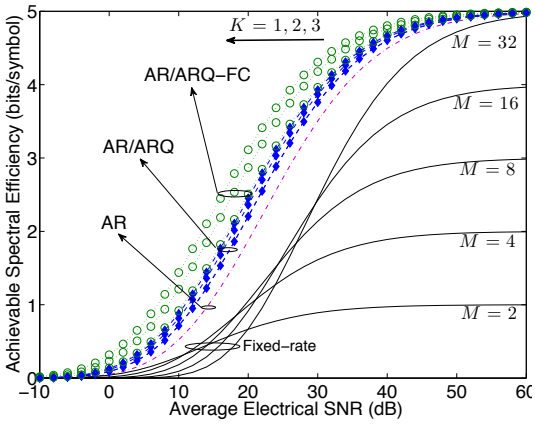

Fig. 3. Achievable spectral efficiency obtained by (28), for fixed-rate, AR, AR/ARQ and AR/ARQ-FC in the weak turbulence condition.

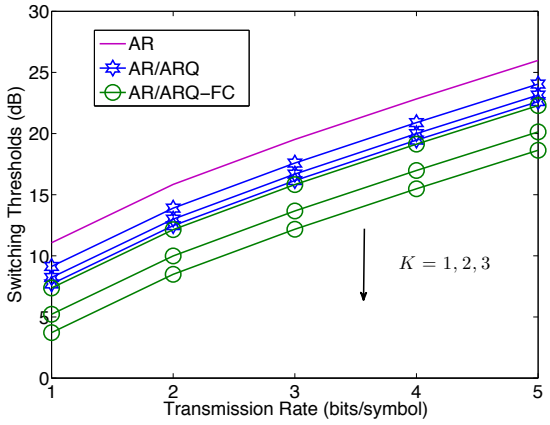

Fig. 4. Switching thresholds, obtained by (8), (16) and (19), for AR, AR/ARQ, and AR/ARQ-FC.

efficiency of 3.5 bits/symbol, compared to the system with fixed-rate system with 32-QAM, the AR system offers more than 5-dB gain.

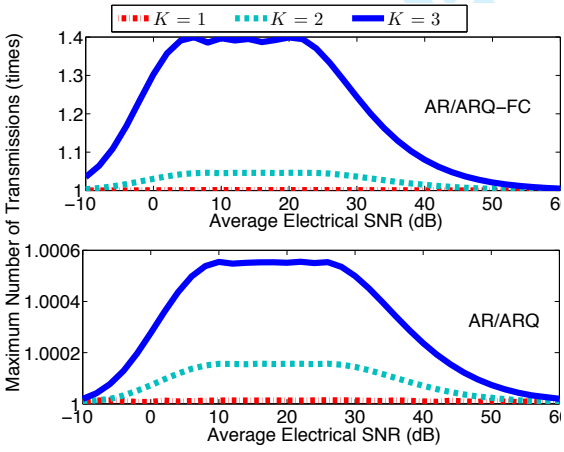

Fig. 5. Maximum expected number of transmissions, obtained by (30), for AR/ARQ and AR/ARQ-FC in the weak turbulence condition.

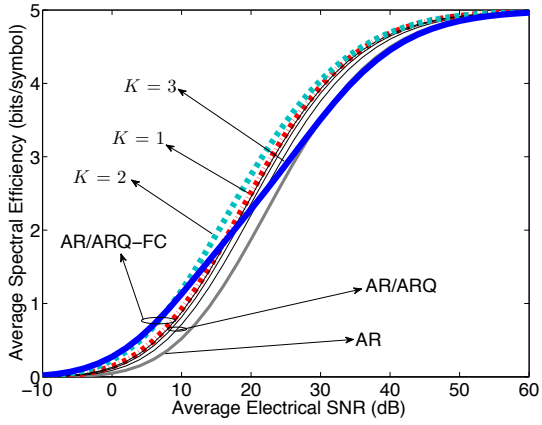

Fig. 6. Average spectral efficiency, obtained by (29), for AR/ARQ and AR/ARQ-FC in the weak turbulence condition.

More importantly, the comparison of adaptive-rate systems shows the cross-layer designs outperform conventional one, and that AR/ARQ-FC has the best performance. Moreover, in cross-layer designs, it is seen that the increase of persistence level further improves spectral efficiency; especially for AR/ARQ-FC the improvement can be seen clearly. In order to explain why there is such phenomenon, we refer back to Section 3. Using (8), (16) and (19), in Fig. 4, the switching thresholds are obtained for different designs. Obviously, by applying cross-layer designs, the thresholds tend to be shifted to lower levels, and when increasing the ARQ persistence level the thresholds are further decreased. Lower threshold levels allow the system to retain a high

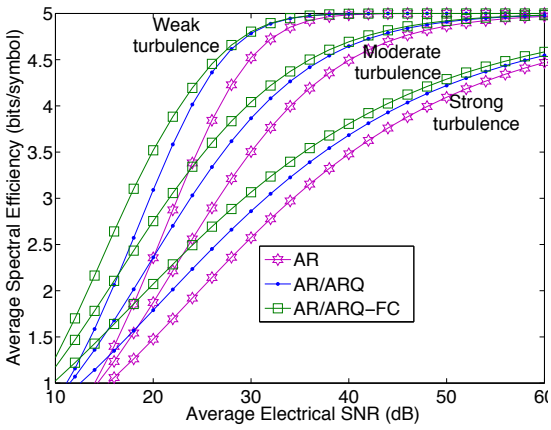

Fig. 7. Average spectral efficiency, obtained by (29), for AR, AR/ARQ, and AR/ARQ-FC in different turbulence conditions.

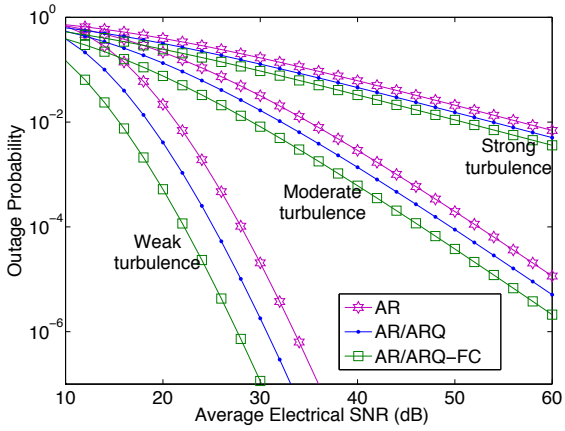

Fig. 8. Outage probability, obtained by (31), for AR, AR/ARQ, and AR/ARQ-FC in different turbulence conditions.

transmission rate when the channel condition gets worse[7], thus resulting in the higher spectral efficiency.

In Fig. 5, we depict the maximum expected number of transmissions, which reflects the costs of using ARQ protocols. This confirms a point that an increase in persistence level results in increasing the average number of transmissions. Moreover, the number of transmissions is relatively high in the case of AR/ARQ-FC with $K = 3$. It is due to the fact that switching thresholds are shifted to very low levels in this persistence level; despite having a good error control capability, operating in such switching thresholds may cause the AR/ARQ-FC system a high frame-error rate, thus resulting in a high number of transmissions.

Consider both Figs. 3 and 5, obviously, higher value of persistence level will result in higher achievable spectral efficiency. This, however, also causes higher number of transmissions. In order to analyze the combined effect of persistence level on both spectral efficiency and number of transmissions, in Fig. 6, we consider the overall spectral efficiency. This is calculated by the ratio between the achievable spectral efficiency and the number of transmissions. Using this metric, we are able to optimize the persistence level for the trade-off between the number of transmissions and the achievable spectral efficiency.

It is intuitively clear in the figure that the increase of K further improves the spectral efficiency; however, the improvement increases slowly, and when $K = 3$ the performance even becomes worse in the case of AR/ARQ-FC. This implies that the persistence level need not be arbitrarily large. A small value of K can achieve sufficient spectral efficiency gain. This also incurs lower delay and energy consumption. Moreover, in the case of AR/ARQ-FC, the small value of K has an additional meaning: it requires a smaller buffer-size penalty at the receiver, thus improving the possibility to implement such design in practical. We therefore highly recommend $K = 2$ for cross-layer designs in practical.

Finally, in Figs. 7 and 8, we analyze the overall spectral efficiency and outage probability when the optimal persistence level $K = 2$ is used for cross-layer designs. The purpose is to find the range of average SNR at which a specific value of system performance is obtained under the impact of different turbulence conditions. As is evident, the atmospheric turbulence greatly affects on the system performance. In particular, an increase of turbulence strength results in an increase

[7]When the channel condition gets worse, the instantaneous received SNR decreases. The system however still stays in the current transmission rate as long as the SNR is higher than the switching threshold. With low switching thresholds, the system has more chances to stay in current rate.

of the required SNR to achieve the same performance. For example, in order to obtain an average spectral efficiency of 3.5 bits/symbol, the required SNRs for the system with AR/ARQ-FC are 20 dB, 27 dB and 39 dB corresponding to weak, moderate and strong turbulences, respectively. In the case of outage probability, the probability is relatively high in the strong turbulence condition. Both figures also confirm that, in all atmospheric turbulence conditions, the overall system performance can be significantly improved by employing cross-layer designs with the optimal persistence level.

6. Conclusions

This paper developed a cross-layer framework incorporating AR transmission with ARQ. By fully exploiting the cross-layer gain, switching thresholds were designed to maximize the spectral efficiency under prescribed QoS requirements. Two cross-layer designs, including AR/ARQ and AR/ARQ-FC, were discussed. The Markov chain models were presented to theoretically analyze the system performance. The results shown that compared to the conventional systems, the systems employing cross-layer designs have significantly better spectral efficiency and transmission reliability, and among cross-layer designs AR/ARQ-FC in general performs more efficiently than AR/ARQ. In addition, the optimal persistence level was investigated to maximize the spectral efficiency, while minimizing the number of transmissions. It was found that the recommended value of persistence level is 2 for the cross-layer designs. Numerical results showed that the impact of turbulence on the system performance is severe. However, using cross-layer designs with the optimal persistence level could significantly improve overall performance. Through the results, we also showed how to find the range of average SNR at which a specific value of system performance is obtained under the impact of different turbulence conditions.

Appendix
Derivations of $P_i(k)$

First, we consider the case of ARQ with frame combining. The average FER corresponding to the AR state of i and the ARQ state of k can be computed as

$$P_i^{\text{ARQ-FC}}(k) = \frac{1}{p_i}\int_{\gamma_i}^{\gamma_{i+1}} \text{FER}(2^i, k\gamma) f_\gamma(\gamma) d\gamma = \frac{1}{p_i}(\wp(\gamma_{i+1}) - \wp(\gamma_i)), \tag{34}$$

where $\wp(x) = \int_0^x \text{FER}(2^i, k\gamma) f_\gamma(\gamma) d\gamma$. Using a series expansion of the modified Bessel function of second kind given in [31], we rewrite $f_\gamma(\gamma)$ as

$$f_\gamma(\gamma) = \frac{B(\alpha-\beta, 1-\alpha+\beta)}{2\Gamma(\alpha)\Gamma(\beta)} \sum_{p=0}^{\infty} [\frac{a_p(\alpha,\beta)}{\bar{\gamma}^{\frac{p+\beta}{2}}} \gamma^{\frac{p+\beta-2}{2}} - \frac{a_p(\beta,\alpha)}{\bar{\gamma}^{\frac{p+\alpha}{2}}} \gamma^{\frac{p+\alpha-2}{2}}], \tag{35}$$

where $a_p(x,y) = (xy)^{p+y}/[\Gamma(p-x+y+1)p!]$. By substituting (35) and (10) into $\wp(x)$, making the change of variable $t = g\gamma$ with $g = 3k/[2(2^i-1)]$, and then applying the lower incomplete Gamma function, $\Gamma_l(m,k) = \int_0^k t^{m-1}e^{-t}dt$, we can obtain

$$\wp(x) = \frac{0.2lB(\alpha-\beta, 1-\alpha+\beta)}{2g^{\frac{\beta+\alpha}{2}}\Gamma(\alpha)\Gamma(\beta)} \sum_{p=0}^{\infty} [\frac{a_p(\alpha,\beta)}{\bar{\gamma}^{\frac{p+\beta}{2}}} \Gamma_l(\frac{p+\beta}{2}, gx) - \frac{a_p(\beta,\alpha)}{\bar{\gamma}^{\frac{p+\alpha}{2}}} \Gamma_l(\frac{p+\alpha}{2}, gx)]. \tag{36}$$

Finally, substituting (36) to (34), we achieve $P_i^{\text{ARQ-FC}}(k)$. In the case of standard-ARQ, without frame combining, the average FER corresponding to the k-th transmission can be computed as one corresponding to the first transmission of ARQ with frame combining:

$$P_i^{\text{ARQ}}(k) = P_i^{\text{ARQ-FC}}(1). \tag{38}$$

References

[1] D. Kedar and S. Arnon, "Urban optical wireless communication networks: the main challenges and possible solutions," *IEEE Commun. Mag.*, vol. 42, no. 5, pp. S2–S7, May 2004.
[2] M. Khalighi and M. Uysal, "Survey on free space optical communication: A communication theory perspective," *IEEE Commun. Surveys Tuts.*, vol. 16, no. 4, pp. 2231–2258, Fourthquarter 2014.
[3] L. C. Andrews, R. L. Phillips, C. Y. Hopen, and M. A. Al-Habash, "Theory of optical scintillation," *J. Opt. Soc. Am. A*, vol. 16, no. 6, pp. 1417–1429, June 1999. [Online]. Available: http://josaa.osa.org/abstract.cfm?URI=josaa-16-6-1417
[4] R. L. P. L. C. Andrews and C. Y. Hopen, *Laser Beam Scintillation with Applications*. Bellingham, WA: SPIE, 2001.
[5] M. A. Al-Habash, L. C. Andrews, and R. L. Phillips, "Mathematical model for the irradiance probability density function of a laser beam propagating through turbulent media," *Opt. Eng.*, vol. 40, no. 8, pp. 1554–1562, 2001. [Online]. Available: http://dx.doi.org/10.1117/1.1386641
[6] A. K. Majumdar, "Free-space laser communication performance in the atmospheric channel," *J. Opt. Fiber Commun. Rep.*, vol. 2, no. 4, pp. 345–396, 2005. [Online]. Available: http://dx.doi.org/10.1007/s10297-005-0054-0
[7] I. Djordjevic, "Adaptive modulation and coding for free-space optical channels," *IEEE/OSA J. Opt. Commun. Netw.*, vol. 2, no. 5, pp. 221–229, May 2010.
[8] A. García-Zambrana, C. Castillo-Vázquez, and B. Castillo-Vázquez, "Rate-adaptive fso links over atmospheric turbulence channels by jointly using repetition coding and silence periods," *Opt. Express*, vol. 18, no. 24, pp. 25 422–25 440, Nov. 2010.
[9] N. Chatzidiamantis, A. Lioumpas, G. Karagiannidis, and S. Arnon, "Adaptive subcarrier psk intensity modulation in free space optical systems," *IEEE Trans. Commun.*, vol. 59, no. 5, pp. 1368–1377, May 2011.
[10] M. Hassan, M. Hossain, and J. Cheng, "Performance of non-adaptive and adaptive subcarrier intensity modulations in gamma-gamma turbulence," *IEEE Trans. Commun.*, vol. 61, no. 7, pp. 2946–2957, July 2013.
[11] K. Kiasaleh, "Hybrid arq for fso communications through turbulent atmosphere," *IEEE Commun. Lett.*, vol. 14, no. 9, pp. 866–868, Sept. 2010.
[12] S. Aghajanzadeh and M. Uysal, "Information theoretic analysis of hybrid-arq protocols in coherent free-space optical systems," *IEEE Trans. Commun.*, vol. 60, no. 5, pp. 1432–1442, May 2012.
[13] E. Zedini, A. Chelli, and M.-S. Alouini, "On the performance analysis of hybrid arq with incremental redundancy and with code combining over free-space optical channels with pointing errors," *IEEE Photon. J.*, vol. 6, no. 4, pp. 1–18, Aug. 2014.
[14] V. V. Mai and A. T. Pham, "Performance analysis of cooperative-arq schemes in free-space optical communications," *IEICE Trans. Commun.*, vol. E97-B, no. 8, pp. 1614–1622, Aug. 2014.
[15] Q. Liu, S. Zhou, and G. Giannakis, "Cross-layer combining of adaptive modulation and coding with truncated arq over wireless links," *IEEE Trans. Wireless Commun.*, vol. 3, no. 5, pp. 1746–1755, Sept. 2004.
[16] J. Harsini, F. Lahouti, M. Levorato, and M. Zorzi, "Analysis of non-cooperative and cooperative type ii hybrid arq protocols with amc over correlated fading channels," *IEEE Tran. Wireless Commun.*, vol. 10, no. 3, pp. 877–889, Mar. 2011.
[17] Y. Yang, H. Ma, and S. Aissa, "Cross-layer combining of adaptive modulation and truncated arq under cognitive radio resource requirements," *IEEE Trans. Vehicular Techno.*, vol. 61, no. 9, pp. 4020–4030, Nov. 2012.
[18] J. Choi and J. Ha, "On the energy efficiency of amc and harq-ir with qos constraints," *IEEE Trans. Vehicular Techno.*, vol. 62, no. 7, pp. 3261–3270, Sept. 2013.
[19] Hlawatsch, Franz, and G. Matz, *Wireless Communications Over Rapidly Time-Varying Channels*, 1st ed. Academic Press, 2011.
[20] V. V. Mai, T. C. Thang, and A. T. Pham, "Cross-layer design and analysis for fso links using automatic repeat request and adaptive modulation/coding schemes," in *Proc. IEEE/IET CSNDSP*, July 2014, pp. 1176–1180.
[21] V. V. Mai and A. T. Pham, "Adaptive multi-rate designs for hybrid fso/rf systems over fading channels," in *Proc. IEEE GLOBECOM WS-OWC*, Dec. 2014, pp. 554–559.
[22] R. Barrios and F. Dios, *Wireless Optical Communications through the Turbulent Atmosphere: A review*. Chapter 1, Narottam Das, InTech, 2012.
[23] D. Giggenbach, W. Cowley, K. Grant, and N. Perlot, "Experimental verification of the limits of optical channel intensity reciprocity," *Appl. Opt.*, vol. 51, no. 16, pp. 3145–3152, June 2012.
[24] B. Teipen, M. Eiselt, K. Grobe, and J.-P. Elbers, "Adaptive data rates for flexible transceivers in optical networks," *J. Net.*, vol. 7, no. 5, 2012.
[25] F. Digham and M.-S. Alouini, "Variable-rate variable-power hybrid m-fsk m-qam for fading channels," in *Proc. IEEE VTC-Fall*, vol. 3, Oct. 2003, pp. 1512–1516.
[26] C.-H. Yu, A. Hellsten, and O. Tirkkonen, "Rate adaptation of amc/harq systems with cqi errors," in *Proc. IEEE VTC-Spring*, May 2010, pp. 1–5.
[27] A. Puryear, R. Jin, E. Lee, and V. W. S. Chan, "Experimental analysis of the time dynamics of coherent communication through turbulence: Markovianity and channel prediction," in *Proc. ICSOS*, May 2011, pp. 28–37.
[28] K. Peppas and C. Datsikas, "Average symbol error probability of general-order rectangular quadrature amplitude modulation of optical wireless communication systems over atmospheric turbulence channels," *IEEE/OSA J. Opt. Commun. Netw.*, vol. 2, no. 2, pp. 102–110, Feb. 2010.
[29] H.-S. Wang and N. Moayeri, "Finite-state markov channel-a useful model for radio communication channels," *IEEE Trans. Vehicular Techno.*, vol. 44, no. 1, pp. 163–171, Feb. 1995.
[30] J. Mo, "Performance Modeling of Communication Networks with Markov Chains," *Synthesis Lectures on Data Management*, vol. 3, no. 1, pp. 1–90, 2010.
[31] E. Bayaki, R. Schober, and R. Mallik, "Performance analysis of mimo free-space optical systems in gamma-gamma fading," *IEEE Trans. Commun.*, vol. 57, no. 11, pp. 3415–3424, Nov. 2009.